SECOND EUROPEAN CONFERENCE ON EARTHQUAKE ENGINEERING
AND SEISMOLOGY, ISTANBUL AUG. 25-29, 2014

DISPLACEMENT-BASED SEISMIC DESIGN OF UNREINFORCED MASONRY BUILDINGS

Fulvio PARISI[1] and Nicola AUGENTI[2]

ABSTRACT

Displacement-based seismic design has been proved to be a rational procedure allowing the control of the inelastic response for both framed and wall structures under earthquake loading. Nevertheless, the application of this design methodology to masonry buildings still needs to be investigated.

In this paper, a direct displacement-based design (DDBD) procedure for unreinforced masonry (URM) buildings is presented and critically compared to force-based design (FBD). DDBD was applied to a three-storey brick masonry building, which was assumed to be located in a high-seismicity site in Italy. Analysis results show that: (1) both the combination of horizontal seismic actions and non-zero accidental eccentricities may induce a significant increase and scattering in strength demands on URM shear walls, especially in near-field earthquake conditions; (2) after design optimisation, construction costs resulting from the proposed DDBD procedure may be about 30% lower than those provided by current code-based FBD procedures.

INTRODUCTION

In the last decade, displacement-based seismic design procedures have received great interest because they are more effective than classical force-based design (FBD) approaches in controlling both local and global deformations of structures. For instance, the distribution of earthquake resistance throughout the structure on the basis of equilibrium considerations instead of stiffness-based formulations typically produces a more controlled and predictable seismic response, avoiding undesirable failure modes. Given that deformations are directly correlated with damage, limiting them to threshold levels allow designers to control both safety levels and costs in the lifetime of structures according to performance-based design (PBD) principles (e.g., SEAOC, 1995; ATC, 2006).

Priestley et al. (2007) developed a direct displacement-based design (DDBD) methodology, which was specialised to different types of structures accounting for their specific behavioural features. A model code was also developed by Sullivan et al. (2012). DDBD allows one to design a building so that the overall displacement demand corresponding to a given design earthquake does not exceed displacement capacity, where the latter depends on materials and structural configuration.

Research on DDBD has just partially covered the field of masonry buildings, even though they are widely present in earthquake-prone regions. A displacement-based approach was proposed by Calvi (1999) for vulnerability assessment of masonry building portfolios at regional scale. Recently, a DDBD procedure for single reinforced masonry buildings was proposed and validated through shaking-table tests (Ahmadi et al., 2013a,b).

This paper focuses on the application of DDBD to unreinforced masonry (URM) buildings at site-specific scale. It is assumed that proper detailing is adopted to prevent out-of-plane failure modes

[1] Assistant Professor, University of Naples Federico II, Naples, fulvio.parisi@unina.it
[2] Associate Professor, University of Naples Federico II, Naples, augenti@unina.it

of masonry walls, so the latter are laterally loaded in their own plane providing global earthquake resistance to the URM building. After that FBD is critically reviewed, a DDBD procedure is set up and applied to a three-storey URM building, discussing the effects of load combinations and accidental eccentricities. Finally, construction costs resulting from FBD and DDBD solutions are compared, after design optimisation.

LIMITATIONS OF FORCE-BASED DESIGN FOR URM BUILDINGS

Current seismic codes, such as Eurocode 8 (EC8) (CEN, 2004) and the Italian Building Code (IBC) (IMIT, 2008), use the FBD approach for URM buildings. IBC provides the procedure reported in EC8, while deriving elastic response spectra through a site-specific seismic hazard assessment.

IBC allows one to define a (temporal) reference period V_R and a probability of exceedance P_{VR}, based on the importance and use of the building. Seismic hazard at the building site is estimated in terms of: peak ground acceleration at the bedrock (a_g); maximum amplification factor of the horizontal spectral acceleration (F_o); and upper bound period of the constant spectral acceleration branch on type A ground (T_C^*), i.e., rock or rock-like geological formation. Such hazard parameters are associated with the return period of design earthquake (T_R) which depends on V_R and P_{VR}. According to PBD (SEAOC, 1995), different values of P_{VR} are assigned to serviceability and ultimate limit states (ULSs). V_R is a characteristic parameter of the building, being it defined as the nominal lifetime (V_N) times the importance factor of the structure (C_U). To account for ground motion amplification effects due to local site conditions, a_g is multiplied by a soil factor S which is defined as a stratigraphic amplification factor (S_S) times a topographic amplification factor (S_T). Stratigraphic conditions are also considered when defining the limit periods of the elastic response spectra. Indeed, a soil-related factor C_C is computed and multiplied by T_C^* to define T_C (namely, the upper bound period for soils different from type A) and to derive the other limit periods denoted by T_B and T_D. Therefore, IBC provides elastic response spectra which are different from those reported in EC8, while the same FBD procedure is used. It is emphasised that: (1) the importance of the building is taken into account by V_R into IBC and through an importance factor γ_I into EC8, the latter directly applied to a_g; and (2) EC8 accounts for topographic amplification effects only in the case of important structures ($\gamma_I > 1$) and sets $F_o = 2.5$.

Dealing with seismic demand, a viscous damping ratio equal to 5% and a first-mode vibration period T_1 are assumed for the structure. If the URM building has a rather uniform distribution of mass along the height, T_1 may be set to $0.05H^{3/4}$ where H is the building height (alternative formulations are provided by EC8). Then, the horizontal acceleration demand $S_a(T_1)$ at the base of the building is estimated through the elastic response spectrum. The design acceleration demand at ULS is defined as $S_d(T_1) = S_a(T_1)/q$, where q is the strength reduction (or behaviour) factor of the building. This factor is given by $q = q_0 K_R$, where: q_0 is the maximum strength reduction factor associated with presumed ductility and overstrength levels in the structure; and K_R is a reduction factor accounting for building irregularity in elevation. IBC provides $q_0 = 2\alpha_u/\alpha_1$ in the case of URM buildings, where: α_1 is the horizontal load multiplier associated with the attainment of lateral strength in the weakest wall; α_u is 90% of the horizontal load multiplier associated with the peak resisting force of the building; and α_u/α_1 is the system overstrength factor assumed to be 1.4 and 1.8 for single-storey and multi-storey URM buildings, respectively. In the case of in-plan irregular URM buildings, IBC allows one to set α_u/α_1 as average of the value recommended for in-plan regular buildings and unity. Conversely, EC8 allows the use of a unique behaviour factor $q = 1.5$ in the case of URM buildings designed only for gravity loads and $q = 1.5$–2.5 in the case of URM buildings designed for earthquake resistance.

The design base shear is then computed and vertically distributed according to the tributary inertia masses of the floors and first-mode displacement profile, which is linearised into IBC. The horizontal force at each floor level is applied to the centre of mass C_M and distributed among URM walls in proportion to their lateral stiffness. The latter should be defined considering masonry cracking, whose amount depends on the magnitude of loads. To account for spatial variation of seismic ground motion and uncertainty in the location of inertia masses, an accidental eccentricity $e_a \geq \pm 0.05L$ is assigned to the nominal location of C_M where L is the floor dimension perpendicular to the direction of seismic action. It is noted that the same magnitude and sign are given to e_a at all floor levels. Furthermore, the effects of horizontal seismic components along two perpendicular directions

are combined considering a factor equal to ±1 and ±0.3 for primary and secondary action, respectively.

URM walls are designed so that strength demand does not exceed the factored capacity, according to the load-resistance factor design. In this respect, capacity design is not allowed for URM buildings, because shear and bending capacities cannot be independently modified without changing the aspect ratios of masonry walls. Finally, inelastic displacements are estimated as elastic displacements resulting from linear structural analysis multiplied by a displacement amplification factor μ_d associated with q, T_1 and T_C. Displacement demand is then compared to displacement capacity. If the displacement demand-to-capacity (DCR) ratio exceeds unity, the lateral stiffness of the walls is modified and the FBD procedure is repeated until $DCR \leq 1$ is reached in any wall. Local and global ductility/displacement verifications may be avoided if design rules of the building type under consideration are applied.

In the case of URM buildings, the FBD procedure is affected by several major limitations, as follows:

1) T_1 is assumed to be independent on the actual three-dimensional (3D) configuration and lateral stiffness of the structure. This assumption may significantly influence seismic demand.
2) The q-factor is assumed to be independent on T_1, opposed to research findings for short-period structures (e.g., Miranda and Bertero, 1994). Low energy dissipation levels in URM buildings with significant rocking behaviour of walls should also be considered when assuming the q-factor. In addition, α_u/α_1 should be defined on the basis of the actual structural configuration, considering a sufficient number of URM building types.
3) Lateral stiffness is assumed to be independent on the lateral strength of walls and is reduced up to 50% according to EC8 (CEN, 2004) and IBC (IMIT, 2008), regardless of the axial load level and masonry type. Nonlinear moment–curvature analyses have shown that both the bending curvature at the elastic limit and curvature ductility of URM sections significantly change under varying axial load (Parisi and Augenti, 2010). Wrong assumptions for lateral stiffness may result in unlikely distributions of seismic demand among walls. In the case of nonlinear structural systems, seismic demand always depends on capacity and this particularly applies to URM buildings because of their nonlinear behaviour even in the elastic range. Even if the stiffness of walls is iteratively estimated considering its relation with strength through force–displacement diagrams (e.g., Parisi, 2010), the first two limitations still remain unsolved. As a result, the design solution is not consistent with the real seismic response of the URM building. In the case of walls with openings, the stiffness-based distribution of seismic forces induces strength demand concentrations on stiffer components, strongly limiting their ductility capacity. This may induce extremely different ductility demands throughout the wall and a large error in the q-factor assumed for the entire structural system on the basis of its expected ductility capacity.

DDBD PROCEDURE FOR UNREINFORCED MASONRY BUILDINGS

To overcome the limitations of FBD, a DDBD procedure according to the general methodology by Priestley et al. (2007) is presented, considering accidental eccentricities and different combinations of horizontal actions at each floor level.

Dealing with 3D wall systems, DDBD should account for (1) the displacement profile along the height of the building at maximum response, which corresponds to the first inelastic vibration mode, and (2) the reduction of the target displacement Δ_d as a result of torsional response. The latter depends on the eccentricity e_V between C_M and the centre of strength C_V.

In the case of URM buildings, which are torsionally restrained systems, the lateral strength of walls may be assumed to be known at the beginning of the design procedure. In the presence of non-zero eccentricity, Δ_d is to be reduced so that the wall subjected to the maximum displacement demand due to torsional response does not exceed its displacement capacity. Nevertheless, an accurate design procedure is required to control the inelastic response of the structure. The DDBD procedure proposed in this study consists of several steps which are discussed below.

Step 1: Define the building characteristics. Based on current code rules at both national and international levels (CEN, 2004; IMIT, 2008), URM buildings should be composed of load-bearing

walls with proper masonry interlocking at their intersections, lintels above openings, and reinforced concrete (RC) bond beams at each floor level. Floor systems should be sufficiently stiff and resistant in their own plane with proper connection to masonry walls, in order to distribute horizontal seismic actions in plan. This allows one to expect a box-type global seismic response of the URM building, which the in-plane lateral behaviour of walls is activated. Geometric limitations for walls and RC bond beams, as well as the type and minimum strengths for masonry and reinforcement, are provided by codes. Nonetheless, the structural geometry also depends on architectural choices and expected costs.

Step 2: Perform a macro-element modelling of the structure, defining both strengths and equivalent damping ratios of macro-elements. A macro-element idealisation of masonry walls with openings may be carried out provided that the opening distribution is not significantly irregular (Parisi and Augenti, 2013). In this case, one can identify *spandrels* and *piers*, which are the horizontal and vertical masonry strips between consecutive sets of openings, respectively (Fig. 1). Intersections between spandrels and piers delineate *joint panels*, which are typically assumed to be rigid macro-elements. Conversely, two types of flexible macro-elements are defined: *pier panels*, namely the vertical structural components between consecutive openings and joint panels; *spandrel panels*, namely the horizontal structural components between consecutive piers (Parisi, 2010).

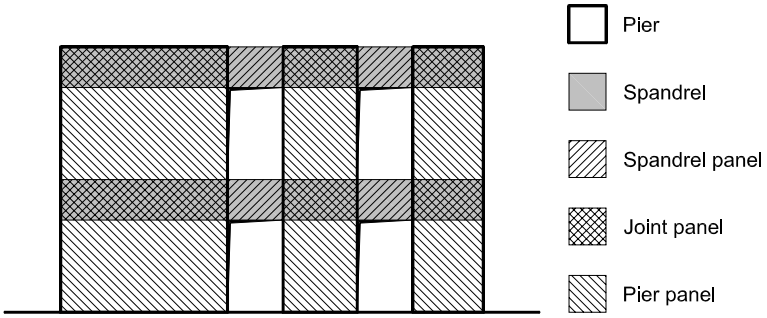

Figure 1. Macro-element idealisation of URM wall with openings

Both pier and spandrel panels may fail in bending or shear, depending on their size, boundary conditions and masonry properties (i.e., strength and ultimate strain). Several formulations allow one to predict the in-plane lateral strength of macro-elements (see for instance Parisi, 2010). Opposed to the case of RC and steel framed structures, elastic deformations of URM walls may be neglected when computing the drift capacity θ_u. The latter can typically be set to 0.8% in the case of flexural failure and 0.4% in the case of diagonal tension cracking or diagonal shear sliding. Bed joint sliding failure is not considered for new URM buildings, because it occurs when the strength of masonry units (i.e., stones, bricks or blocks) is significantly greater than that of mortar.

Experimental tests have shown that hysteretic damping changes with the failure mode, resulting in a hysteretic damping ratio ξ_{hys} equal to 5% and 20% in the case of flexural and diagonal shear failure, respectively (Magenes and Calvi, 1997). If the elastic damping ratio ξ_{el} is set to 5%, the equivalent damping ratio $\xi_e = \xi_{el} + \xi_{hys}$ turns out to be 10% and 15% in the case of flexural and diagonal shear failure, respectively. Radiation damping from rocking is generally negligible.

Step 3: Assume a global collapse mechanism for URM walls and cracked spandrels. Shear failure of piers has to be avoided since it induces soft storey mechanisms, and hence low displacement capacity even though higher equivalent damping ratios may be assumed. This motivates the assumption of global collapse mechanism which results from cracking of spandrels and rocking behaviour of piers. The latter are assumed to experience a rigid-body rotation so the drift demand on spandrels θ_S is larger than that on piers θ_P according to the following equation:

$$\theta_S = \theta_P \left(1 + \frac{l_P}{l_S} \right) \tag{1}$$

where l_P and l_S are the lengths of the pier and spandrel panel, respectively (Fig. 2a). Eq. (1) was also assessed by Parisi et al. (2013) after numerical simulations of lateral loading tests on a URM wall with single opening. The pier drift θ_P is set equal to the target (design) drift θ_d and the contribution of spandrels to coupling is considered if l_S is significantly larger than l_P so that $\theta_S \leq 1.5\theta_d$. In the case of piers and spandrels with different lengths, Eq. (1) may be generalised to:

$$\theta_{S,ij} = \theta_P \left(1 + \frac{l_{P,i} + l_{P,j}}{2l_{Sij,eff}} \right) \tag{2}$$

where: i and j are consecutive piers; $l_{S,ij,eff}$ is an extended effective length of the spandrel panel between piers i and j, which takes into account the curvature penetration within piers. This effective length is a function of the spandrel sectional depth $h_{S,ij}$ and may be assumed to be $l_{S,ij,eff} = l_{S,ij} + 2h_{S,ij}$. Therefore, after that θ_d is assigned to piers, one can predict the rotation demand on spandrels assuming that it is uniform along the building height.

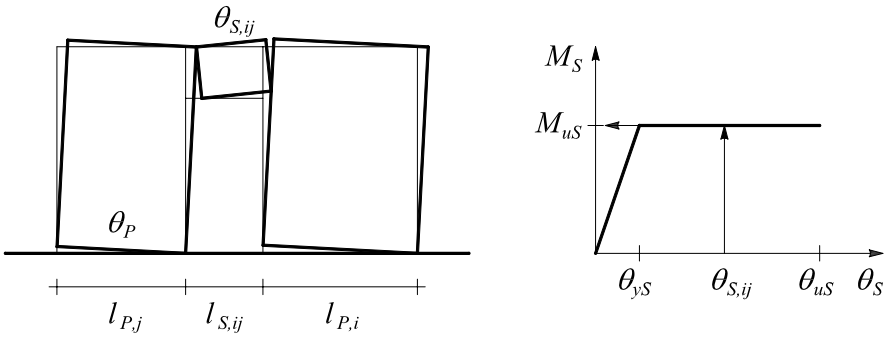

Figure 2. Demand measures on a spandrel panel: (a) rotation; (b) bending moment

Step 4: Check the pier coupling provided by spandrels at each floor level. As far as the seismic response of URM walls with openings is concerned, spandrels play an important role because they provide coupling between piers. Coupling effectiveness depends on the presence of RC bond beams, floor slabs or just masonry within spandrels. Coupling is influenced by geometric conditions, force equilibrium and strength of elements within spandrels. Based on rotation demand provided by Eq. (1) or (2), the bending moment transmitted by spandrels to piers can be predicted through the moment–rotation relationship assumed for spandrels (Fig. 2b).

If the spandrel includes a RC bond beam or floor slab, its yielding rotation may be computed considering 10% contribution from shear deformation, as follows:

$$\theta_{yS} = 0.35\varepsilon_y \frac{l_{S,eff}}{h_b} \tag{3}$$

where: ε_y is the yielding strain of reinforcing steel; $l_{S,eff}$ is the effective length of the spandrel panel; h_b is the bond beam height. If a bilinear moment–rotation diagram is assumed, the bending moment transmitted by the spandrel to the pier is $M_S = M_{uS}$ if $\theta_S \geq \theta_{yS}$ and $M_S = M_{uS}\theta_S/\theta_{yS}$ if $\theta_S < \theta_{yS}$.

If the spandrel includes a floor slab, the bending moment may be calculated assuming that the effective width of the floor slab is 3 times the thickness of the supporting wall.

The fraction of overturning moment carried by spandrels is quantified by the coupling ratio:

$$\beta_S = \frac{\sum_{i=1}^{n} M_{S,i}}{M_{OTM}} \tag{4}$$

where: n is the number of floor levels; $M_{S,i}$ is the bending moment transmitted by spandrels to piers at the i-th floor level; M_{OTM} is the overturning moment. Bending moments and shear forces transmitted by spandrels increase the earthquake resistance of the building, increasing damping and stiffness of walls, and changing the contraflexure height H_{cf}. However, in the case of URM walls with openings, the coupling degree mainly depends on characteristics of floor slabs and RC bond beams.

The maximum degree of coupling depends on the balance between flexural and shear strengths of spandrels and vertical loads carried by piers and spandrels. The shear forces corresponding to the bending moments of spandrels may be computed through equilibrium equations, so the actual coupling degree must be compatible with the following equilibrium condition at each floor level (Fig. 3a):

$$\frac{M_{S,l} + M_{S,r}}{l_P} + \frac{V_{S,l} + V_{S,r}}{2} \le W_P + \frac{W_S}{2} \tag{5}$$

where: $M_{S,l}$ and $V_{S,l}$ are the bending moment and shear at the left section of the spandrel panel; $M_{S,r}$ and $V_{S,r}$ are the bending moment and shear at the right section of the spandrel panel; W_P and W_S are the vertical loads acting on the pier and spandrel panel, respectively, including self-weight and tributary loads transferred by the floor. If Eq. (5) is not met (typical case of upper floor levels), the bending moments and shear forces transmitted by the spandrel are reduced in proportion to the unbalance level before β_S is computed through Eq. (4). The coupling action of spandrels induces axial load variations ΔN in piers, which are equal to the shear forces transmitted by spandrels. The total axial load at the base of coupled piers is then equal to $N = N_G \pm \Delta N$ where: N_G is the axial force due to gravity loads; $\Delta N = \Sigma V_{S,i}$ with $i = 1 \ldots n$ (Fig. 3b).

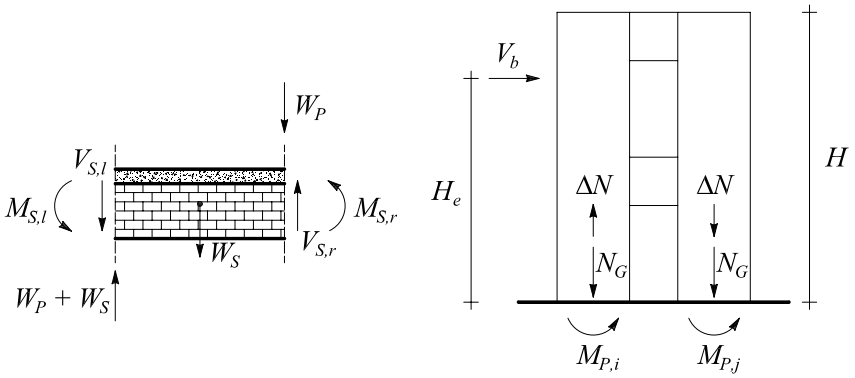

Figure 3. (a) Equilibrium condition of the spandrel panel; (b) axial loads in piers

If the spandrel has no RC bond beams or floor slabs, its coupling action simply results from the formation of a diagonal compression strut within the masonry. This resisting mechanism is limited by the masonry compressive strength parallel to bed joints (horizontal direction), which may be much lower than compressive strength perpendicular to bed joints (vertical direction). If the compression strut develops within masonry, Eqs. (4) and (5) still apply. If the spandrel includes a lintel well bonded to the piers above openings, M_S reaches its peak value at the end section of the spandrel panel where the maximum internal lever arm is attained, and is almost zero at the opposite end section.

Step 5: Evaluate the contraflexure and effective heights. According to Priestley et al. (2007), the ratio of the effective height H_e to the building height H may be estimated as function of the number of storeys n. If the URM building has 2 or 3 storeys, it may be assumed $H_e = 0.8H$. Besides, H_{cf} may be estimated as function of β_S. The following equation was derived by nonlinear regression (coefficient of determination $R^2 = 0.975$):

$$H_{cf} = \left(-0.92\beta_S^2 - 0.36\beta_S + 1.06\right)H \tag{6}$$

Step 6: Check the assumed global collapse mechanism and evaluate the effective mass of the equivalent SDOF system. The shear force corresponding to flexural failure of the spandrel should not exceed that related to diagonal shear failure, that is $V_f \leq V_s$. If this occurs, the assumption of global collapse mechanism is confirmed. Otherwise, a soft-storey mechanism is expected so the equivalent damping ratio and design drift are respectively set to 15% and 0.4%. The effective mass is defined as:

$$m_e = \frac{\sum_{i=1}^{n} m_i \Delta_i}{\Delta_d} \tag{7}$$

and may typically be set to 90% of total mass, assuming a linear displacement profile. This allows one to define m_e before Δ_d is estimated.

Step 7: Define the equivalent damping ratio of the building. Neglecting the coupling action of spandrels would be overly conservative to estimate the equivalent damping ratio of the overall structural system. This also applies in the case of URM buildings where the coupling ratio is typically $\beta_S \leq 0.5$, because of the higher ductility demands on spandrels compared to piers.

In the general case of systems composed of m lateral-load resisting elements with different lateral strength and damping, the equivalent damping ratio ξ_e may be defined as weighted average based on the energy dissipated by the elements, namely:

$$\xi_e = \frac{\sum_{j=1}^{m} V_{b,j} \Delta_j \xi_{e,j}}{\sum_{j=1}^{m} V_{b,j} \Delta_j} \tag{8}$$

where $V_{b,j}$, Δ_j, and $\xi_{e,j}$ are respectively the design base shear at the design displacement, the displacement at height of centre of seismic force, and the equivalent damping ratio of the j-th element (note that the dissipated energy is related to plastic hinge moment and rotation in framed structures).

Given that the failure modes of piers and walls without openings are assessed in Step 6, the equivalent damping ratio of those elements is known, namely, 10% in the case of flexural failure and 15% in the case of shear failure. Conversely, the equivalent damping ratio of the spandrel may be estimated according to the ξ_e–μ relationship associated with "Takeda fat" hysteretic model, as follows:

$$\xi_S = 0.05 + 0.565\left(\frac{\mu - 1}{\mu\pi}\right) \tag{9}$$

where μ is the ductility demand on spandrel, that is, $\mu = \theta_S/\theta_{yS}$ if $\theta_S \geq \theta_{yS}$ and $\mu = 1$ if $\theta_S < \theta_{yS}$. In the case of multiple spandrels, Eq. (9) is applied considering the average ductility demand. Therefore, accounting for the coupling action of spandrels, the equivalent damping ratio of an entire URM wall with openings may be defined by:

$$\xi_e = \left(1 - \beta_S\right)\xi_P + \beta_S \xi_S \tag{10}$$

where ξ_P is the equivalent damping ratio of piers. If the spandrel strength is not uniform over the building height, Eq. (10) may be generalised assuming ξ_S as weighted damping ratio based on bending moments transmitted by spandrels.

Step 8: Determine the target displacement accounting for drift limits of piers and torsional response of the structure. If the building structure is expected to experience no torsional response, the target displacement may be directly assumed to be $\Delta_d = \theta_P H_e$. A reduction in target displacement is

induced by the torsional rotation. To account for storey torsion, the components of strength eccentricity e_V in the principal directions have first to be determined as follows:

$$e_{Vx} = \frac{\sum_{i=1}^{n} V_{y,i} x_i}{\sum_{i=1}^{n} V_{y,i}} \qquad e_{Vy} = \frac{\sum_{i=1}^{n} V_{x,i} y_i}{\sum_{i=1}^{n} V_{x,i}} \tag{11}$$

where $V_{x,i}$ and $V_{y,i}$ are the lateral resisting forces of walls in the *x*- and *y*-direction of the building plan, respectively. A conservative estimate of torsional stiffness may be predicted as follows:

$$J_{R,V} = \sum_{i=1}^{n} k_{y,i} \left(x_i - e_{Vx} \right)^2 + \sum_{i=1}^{n} k_{x,i} \left(y_i - e_{Vy} \right)^2 \tag{12}$$

assuming that every wall fails in flexure and its effective lateral stiffness is proportional to strength, namely, $k_{eff,i} = V_i/\Delta_d$. This assumption is acceptable if the torsional rotation is reasonably small and implies the full inelastic response simultaneously in both principal directions.

The torsional rotation demand in each direction is then given by:

$$\theta_{n,x} = \frac{V_{b,x} e_{Vy}}{J_{R,V}} \qquad \theta_{n,y} = \frac{V_{b,y} e_{Vx}}{J_{R,V}} \tag{13}$$

where $V_{b,x}$ and $V_{b,y}$ are the design base shear forces in such directions. Finally, the design displacement of C_M in each direction can be reduced as follows:

$$\Delta_{d,x} = \theta_P H_e - \theta_{n,x} \left(y_{i,\max} - e_{Vy} \right) \qquad \Delta_{d,y} = \theta_P H_e - \theta_{n,y} \left(x_{i,\max} - e_{Vx} \right) \tag{14}$$

Priestley et al. (2007) do not recommend consideration of accidental eccentricity in DDBD, since it implicates an increase in strength capacity of all structural elements, resulting in torsional moment amplification and minor effects including a reduction in displacements. Nonetheless, the effects of accidental eccentricity on DDBD of URM buildings are assessed in this study.

Step 9: Define the design earthquake through seismic hazard disaggregation. Seismic hazard at the building site should be disaggregated in terms of source-to-site distance R and moment magnitude M_w, to assess the design earthquake(s) providing the highest contribution to the probability of exceeding a prescribed level of peak ground acceleration within the reference period V_R.

Step 10: Derive both elastic and over-damped displacement response spectra. Based on the design earthquake(s) derived by seismic hazard disaggregation, one may derive the elastic response spectrum corresponding to $\xi_{el} = 5\%$. This spectrum is characterised by the corner period (in s):

$$T_D = 1.0 + 2.5\left(M_w - 5.7 \right) \qquad \text{if } M_w > 5.7 \tag{15}$$

(denoted by T_C in Priestley et al., 2007) and the corresponding spectral displacement (in mm):

$$\Delta_{D,5} = C_S \frac{10^{\left(M_w - 3.2 \right)}}{R} \tag{16}$$

where C_S is a local amplification factor related to the soil (Faccioli et al., 2004). The design spectrum may then be defined as over-damped displacement response spectrum considering the following scaling factor reported in a past edition of EC8 (CEN, 1998):

$$R_{\xi} = \left(\frac{0.07}{0.02 + \xi_e} \right)^{\alpha} \tag{17}$$

where $\alpha = 0.5$. This factor may be used to account for the type of design earthquake, assuming $\alpha = 0.25$ if $R < 10$ km (near-field, forward directivity conditions) and $\alpha = 0.5$ if $R > 10$ km (far-field conditions).

Step 11: Evaluate the effective period and stiffness of the SDOF system. Given that two equivalent damping ratios $\xi_{e,x}$ and $\xi_{e,y}$ may be defined for each principal direction separately, two damping-related displacement reduction factors $R_{\xi,x}$ and $R_{\xi,y}$ may be estimated and used to derive the corresponding effective periods and effective stiffness, as follows:

$$T_e = T_D \frac{\Delta_d}{\Delta_{D,5} R_{\xi}} \qquad k_e = m_e \left(\frac{2\pi}{T_e} \right)^2 \tag{18}$$

Step 12: Estimate the design base shear and its distribution among URM walls based on their effective stiffness. Based on lateral stiffness and target displacements derived in previous steps, the design base shear in the *i*-th direction of the building plan may be predicted as $V_{b,i} = k_{e,i} \Delta_{d,i}$.

Step 13: Perform safety verifications and modify structural design if performance objectives are not met or construction costs need to be reduced. The base shear forces in the principal directions may be combined according to different rules depending on the type of design earthquake, that is, pulse-like near-field or ordinary (non-pulse-like near-field or far-field) earthquake. Assuming that horizontal components of the design seismic action are combined as $E_d = \pm\alpha E_x \pm \beta E_y$, α and β may be set to 0.3 and 1, or vice versa, in the case of ordinary earthquake, and both to 1 in the case of pulse-like near-field earthquake. Priestley et al. (2007) state that torsional rotation under diagonal excitation may normally be neglected in DDBD, because on one hand diagonal resistance of the building is typically about 40% greater than that in a principal direction, and on the other hand diagonal displacements of C_M are less than those in the principal directions. This is expected to provide large reserve in displacement capacity to allow for torsional rotation. Nonetheless, the effects of bidirectional seismic input on DDBD of URM buildings are assessed in this paper. For instance, the base shear in the *x*-th direction may be decomposed as $V_{b,x} = V_{b,x}(\delta) + V_{b,x}(e_{Vy}) + V_{b,x}(e_{Vx})$. These three contributions are respectively associated with translation in the *x*-th direction, torsional rotation induced by base shear in the *x*-th direction, and torsional rotation induced by base shear in the *y*-th direction. After that the base shear for each pier is predicted, safety verifications in terms of strength may be carried out. If such verifications are not met, structural geometry and/or strength of walls needs to be modified.

APPLICATION TO A 3-STOREY URM BUILDING

A three-storey residential building assumed to be located in L'Aquila, Italy was designed according to FBD and DDBD procedures. Seismic design was carried out for the ULS of life safety ($P_{VR} = 10\%$ in $V_R = 50$ years), assuming a design earthquake with return period $T_R = 475$ years. The structure was composed of brick masonry walls with openings, one-way RC floor slabs, and RC slabs for stairs. Based on architectural choices, the initial design solution was that shown in Figure 4.

The maximum dimensions in plan were 15.70 m and 17.90 m in the *x*- and *y*-direction, respectively. The interstorey height was set to 3.60 m, so the building height was $H = 10.80$ m. To assess local amplifications of ground motion, a type B ground and horizontal topographic surface T1 were supposed. The nominal properties of brick masonry were as follows: compressive strength $f_{cm} = 6.00$ MPa; yielding strain $\varepsilon_{ym} = 0.25\%$; Young's modulus $E = 6000$ MPa; shear modulus $G = 2400$ MPa; shear strength at zero confining stress $f_{vm} = 0.4$ MPa; friction coefficient $\mu_{fm} = 0.4$; unit weight $\gamma_m = 15$ kN/m^3. Macro-element modelling of URM walls was carried out.

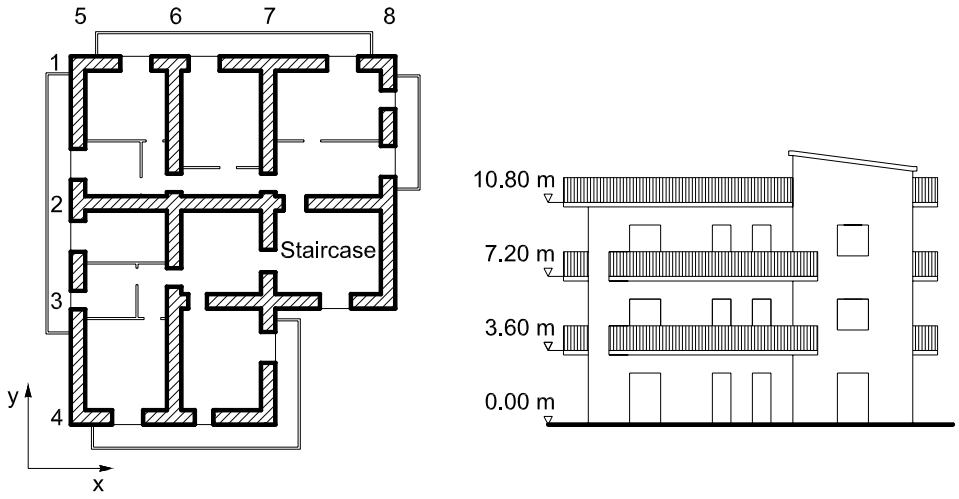

Figure 4. Case-study URM building: (a) plan; (b) lateral view

Flanges resulting from intersections of perpendicular walls were not considered, so every pier was conservatively assumed to have rectangular cross section. RC bond beams were included in spandrels at the height of floors; each beam was assumed to be 150 mm deep with width equal to the wall thickness. RC bond beams were supposed to be made of reinforcing steel type B450C with characteristic yielding strength f_{yk} = 450 MPa and concrete type C20/25 with characteristic cube compressive strength f_{ck} = 25 MPa.

After that a global collapse mechanism was assumed for URM walls, pier coupling was assessed at each floor level by computing the coupling ratio β_S. As expected, the walls were found to be uncoupled at the roof level where spandrels were subjected to an elastic demand. Based on the shear forces transmitted by the RC bond beams, axial load variations on piers were evaluated and bending failure of piers was found. Therefore, the assumption of global collapse mechanism was confirmed and the in-plane lateral strength of walls was that predicted assuming cracked spandrels. Given that the failure mode of piers and the corresponding damping ratio were known, the evaluation of ductility demands on spandrels allowed the estimation of ξ_e for each wall with openings. The properties of walls were then processed to characterise the SDOF system in each direction of the building plan. The target displacement was evaluated in each direction accounting for torsional response. Seismic hazard disaggregation was carried out through REXEL (Iervolino et al., 2010), which allowed to identify a design earthquake with M_w = 6.3 and R = 15 km (Fig. 5a). The corner period and corresponding displacement were then evaluated, deriving two different design displacement spectra on the basis of $R_{\xi,x}$, $R_{\xi,y}$ and α = 0.5 (Fig. 5b). Finally, the computation of effective mass, period and stiffness in each direction provided the corresponding estimates of design base shear, which was distributed among walls and along the height of the building.

Table 1 outlines the maximum percentage variations of design base shear of piers from predictions related to horizontal seismic actions in single directions (that is, α = 0 or β = 0) and zero accidental eccentricity e_a. Major percentage variations were especially found for external walls in case of both far-field and near-field earthquake conditions. In particular, when e_a was set different from zero (see columns 2 and 3), those two earthquake conditions induced different base shear predictions particularly on perimeter walls in the x-direction (i.e., walls 1 and 4). Lower percentage variations were detected when horizontal seismic actions were combined while considering e_a = 0 (see columns 3 and 4). The type of design earthquake significantly affected the magnitude of seismic loads, so different base shear predictions were obtained especially for perimeter walls in the y-direction (i.e., walls 5 and 8). Finally, when both the seismic load combination and accidental eccentricity were taken into account in DDBD, percentage variations of up to 18% and 26% were found in the case of far-field and near-field earthquake conditions. The coefficient of variation of design base shear over all shear walls was found to be 57% and 61% in the case of far-field and near-field earthquake conditions, respectively, reflecting a significant lack of uniformity in the distribution of strength demands.

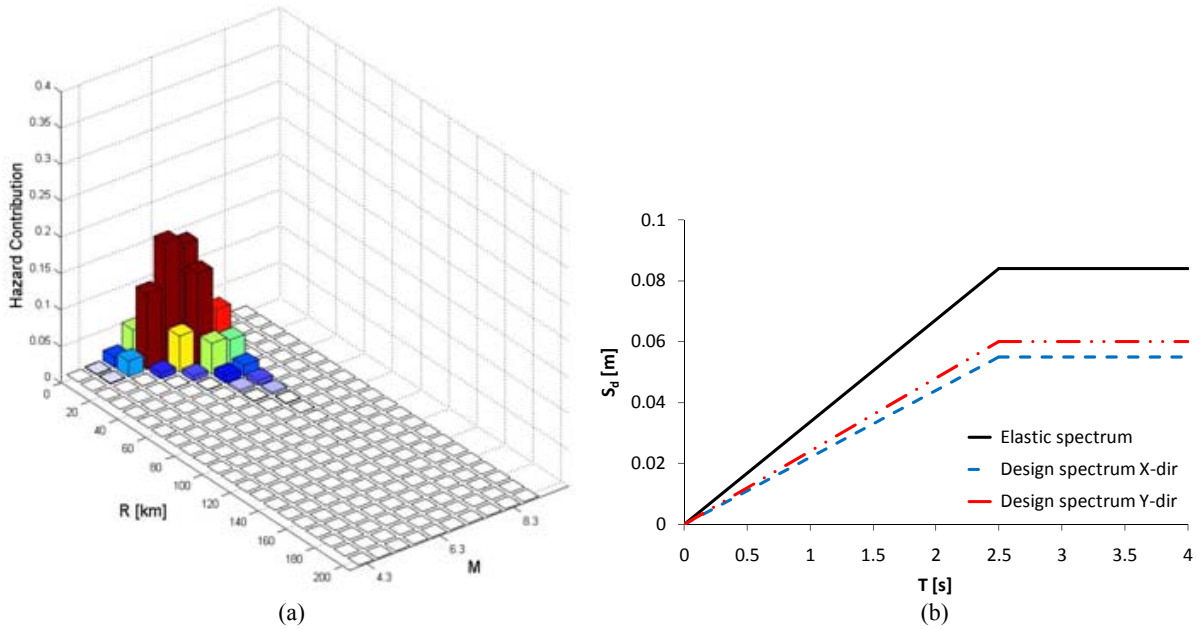

(a) (b)

Figure 5. (a) Seismic hazard disaggregation; (b) displacement response spectra

Table 1. Maximum variations of design base shear of piers provided by DDBD

Wall	$e_a \neq 0$		$\pm\alpha E_x \pm\beta E_y$		$\pm\alpha E_x \pm\beta E_y$ and $e_a \neq 0$	
	Far field	Near field	Far field	Near field	Far field	Near field
1	8%	16%	1%	3%	11%	21%
2	0	1%	0	1%	1%	1%
3	4%	5%	0	2%	5%	8%
4	9%	20%	1%	4%	12%	26%
5	15%	16%	4%	12%	16%	24%
6	5%	6%	1%	3%	5%	7%
7	6%	7%	1%	4%	6%	9%
8	19%	20%	4%	14%	18%	26%

Strength *DCR*s for piers were significantly scattered throughout the building and were notably lower than unity, highlighting the lack of structural optimisation. Indeed, *DCR* ranged between 2% and 71% in the case of zero accidental eccentricity, and between 0 and 79% in the case of 5% accidental eccentricity. Therefore, linear programming was used to maximise *DCR* and its uniformity throughout the structure. A two-step optimisation process was carried out. The first step was aimed at optimising the thickness of shear walls. The second step was performed to optimise the size of piers and openings. The minimum *DCR* resulting from the initial design solution was assumed as objective function. Different bounds were assigned to a number of design variables, as follows: wall thickness t_w = 0.40–0.80 m; pier length $l_P \geq$ 1.20 m; opening length l_O = 0.90–1.80 m. To ensure convergence, a 5% tolerance was accepted for *DCR*, resulting in a maximum allowable *DCR* between 95% and 100%. The same optimisation procedure was applied to FBD, resulting in *DCR* between 21% and 100%. FBD was carried out considering that the building was irregular in both plan and elevation, thus assuming a behaviour factor q = 2.24.

Structural optimisation allowed to estimate construction costs according to standard costs provided by the Abruzzo Region, Italy. FBD led to a construction cost of 279,183 Euros, whereas DDBD led to a cost of 189,482 Euros, resulting in about 32% saving from DDBD.

CONCLUSIONS

A DDBD procedure has been presented and applied to a three-storey brick masonry building. Effects of both the combination of horizontal seismic actions and accidental eccentricities on DDBD have

been assessed. In this regard, horizontal seismic actions were first applied separately in two perpendicular directions of the building plan. After, different load combinations were considered for far-field and near-field design earthquakes. Accidental eccentricity of mass centre at each floor level was set to zero and 5% of plan dimensions, the latter according to EC8 (CEN, 2004).

The analysis of design solutions has shown that: (1) neglecting the combination of horizontal seismic actions and accidental eccentricities within DDBD of URM buildings may result in dangerous underestimations of strength demands on macro-elements, particularly in near-field earthquake conditions; (2) the combination of seismic actions and accidental eccentricities may induce a significant lack of uniformity in the distribution of strength demands on shear walls.

Finally, seismic design was optimised so that safety factors were minimised and construction costs resulting from FBD and DDBD design solutions were estimated for the case-study building. It has been found that DDBD may provide construction costs significantly lower than those resulting from code-based FBD procedures.

REFERENCES

Ahmadi F, Mavros M, Klingner RE, Shing B and McLean D (2013a) "Displacement-based seismic design for reinforced masonry shear-wall structures, Part 1: Background and trial application," *Earthquake Spectra*, DOI: 10.1193/120212EQS344M

Ahmadi F, Mavros M, Klingner RE, Shing B and McLean D (2013b) "Displacement-based seismic design for reinforced masonry shear-wall structures, Part 2: Validation with shake-table tests," *Earthquake Spectra*, DOI: 10.1193/120212EQS345M

American Technology Council (ATC) (2006) FEMA 445 Report: Next-generation performance-based seismic design guidelines program plan for new and existing buildings, Redwood City, USA

Calvi G (1999) "A displacement-based approach for vulnerability evaluation of classes of buildings," *Journal of Earthquake Engineering*, 3(3):411-438

Comité Européen de Normalisation (CEN) (1998) Eurocode 8 - Design of structures for earthquake resistance - Part 1: General rules, seismic actions and rules for buildings, EN 1998-1, Brussels, Belgium

Comité Européen de Normalisation (CEN) (2004) Eurocode 8 - Design of structures for earthquake resistance - Part 1: General rules, seismic actions and rules for buildings, EN 1998-1, Brussels, Belgium

Faccioli E, Paolucci R and Rey J (2004) "Displacement spectra for long periods," *Earthquake Spectra*, 20(2):347-376

Iervolino I, Galasso C and Cosenza E (2010) "REXEL: computer aided record selection for code-based seismic structural analysis," *Bulletin of Earthquake Engineering*, 8(2):339-362

Italian Ministry for Infrastructures and Transportation (IMIT) (2008) DM 14.01.2008: Norme Tecniche per le Costruzioni, Rome, Italy [in Italian]

Magenes G and Calvi GM (1997) "In-plane seismic response of brick masonry walls," *Earthquake Engineering and Structural Dynamics*, 26(11):1091-1112

Miranda E and Bertero VV (1994) "Evaluation of strength reduction factors for earthquake-resistant design," *Earthquake Spectra*, 10(2):357-379

Parisi F (2010) Non-linear seismic analysis of masonry buildings, Ph.D. Thesis, University of Naples Federico II, Naples, Italy [URL: http://wpage.unina.it/fulvio.parisi/]

Parisi F and Augenti N (2010) "Curvature ductility of masonry spandrel panels", *Proceedings of the 14th European Conference on Earthquake Engineering*, Ohrid, FYROM, 30 August - 3 September

Parisi F and Augenti N (2013) "Seismic capacity of irregular unreinforced masonry walls with openings," *Earthquake Engineering and Structural Dynamics*, 42(1):101-121

Parisi F, Lignola GP, Augenti N, Prota A and Manfredi G (2013) "Rocking response assessment of in-plane laterally-loaded masonry walls with openings," *Engineering Structures*, 56:1234-1248

Priestley MJN, Calvi GM and Kowalsky MJ (2007) Displacement-based seismic design of structures, IUSS Press, Pavia, Italy

Structural Engineers Association of California (SEAOC) (1995) Vision 2000: Performance based seismic engineering of buildings, Sacramento, USA

Sullivan TJ, Priestley MJN and Calvi GM (2012) A model code for the displacement-based seismic design of structures, DBD12, IUSS Press, Pavia, Italy